CIRP Journal of Manufacturing Science and Technology 45 (2023) 271–284

Contents lists available at ScienceDirect

CIRP Journal of Manufacturing Science and Technology

journal homepage: www.elsevier.com/locate/cirpj

Novel manufacturing of multi-material component by hybrid friction stir channeling

Heikki Karvinen [a], Kush P. Mehta [b,c], Pedro Vilaça [a,*]

[a] Department of Mechanical Engineering, School of Engineering, Aalto University, Espoo, Finland
[b] Design, Manufacturing and Engineering Management, University of Strathclyde, Glasgow, United Kingdom
[c] LUT Welding Technology, Mechanical Engineering, School of Energy Systems, LUT University, Lappeenranta, Finland

ARTICLE INFO

Article history:
Available online xxxx

Keywords:
Hybrid
Channeling
Weld
Channel
Friction stir
Multi-material
Aluminum alloy
Copper
Dissimilar
Microstructure

ABSTRACT

The hybrid friction stir channeling (HC) is a recent manufacturing technique, reinforcing the broad range of solutions provided by the technological domain of solid-state friction stir-based welding and processing. HC enables the simultaneous welding of multiple components and the sub-surface channeling within the desired region at the stir zone. HC provides new demanding solutions having free path sub-surface channeling and welding for multi-material components with optimized physical and chemical performances. In the present investigation, a multi-material system consisting of 8 mm thick Al-Mg alloy (AA5083) and 3 mm thick oxygen free copper (Cu-OF) was processed by HC. A specially designed tool consists of the probe's body features that steer materials extraction and the probe's tip features that generate materials mixing was applied to produce sub-surface channel at AA5083, along with its simultaneous welding to Cu-OF material. Visual examination of the AA5083's surface processed by the shoulder, cross-sectional dimensioning, optical 3D scanning of the internal surfaces of the channel, optical and scanning electron microscopy, energy dispersive X-ray spectroscopy, electron backscatter diffraction and micro-hardness measurements were applied to investigate the results. The successful application of HC to manufacture multi-material Al-Cu component is demonstrated. A large sub-surface quasi rectangular channel with 9.6 mm in width per 3.3 mm in height was produced in the AA5083 rib along with defect free welding to thin Cu-OF plate at just below the channel region multi-material. The resulted sub-surface channel was consisted of unique wall surface features, with non-uniform and non-oriented surface roughness, suitable to activate turbulent fluid flow. The microhardness field depicts a higher-strength domain of the stirred material, at the ceiling of the sub-surface channel in comparison with the base materials. The welding zone comprises a metal matrix composite structure with Al-Cu inter-mixing and a mechanical hooking from Cu into the Al matrix. The metallurgical features of the weld stirred zone were analyzed, with an interpretation of Al-Cu phases, and solid solution of Al and Cu in each other. In this zone, Cu-rich lamellae regions are dispersed within the Al-matrix, presenting thin layers of discontinuous intermetallic compounds. The effective potential of manufacturing multi-material component for applicability in thermal management system is demonstrated.

Introduction

Hybrid Friction Stir Channeling (HC) [1,2] is a novel friction stir-based manufacturing technique to produce internally closed sub-surface channels with simultaneous welding of multiple metal components that can be similar, or dissimilar, in chemical composition and geometry. The HC process is the only known technique capable of such performance [3]. HC technique opens new design solutions in manufacturing of multi-material components enabling new optimal physical and chemical performances, for high demanding applications where continuous channels along a free path may have a relevant engineering role. Therefore, it can be said that the HC technique combines the best of Friction Stir Welding (FSW) [4–9]and Friction Stir Channeling (FSC) [1,10,11], in a distinct single processing action with its own challenges, benefits and field of application.

Materials with distinct properties, such as aluminum (Al) and copper (Cu), can be processed by HC, considering process features, but not reported in open publications. The Cu is a top performance engineering material in terms of thermal and electrical conductivities, with better corrosion resistance and strength than Al and

* Corresponding author.
E-mail addresses: kush.mehta@strath.ac.uk (K.P. Mehta), pedro.vilaca@aalto.fi (P. Vilaça).

https://doi.org/10.1016/j.cirpj.2023.07.001

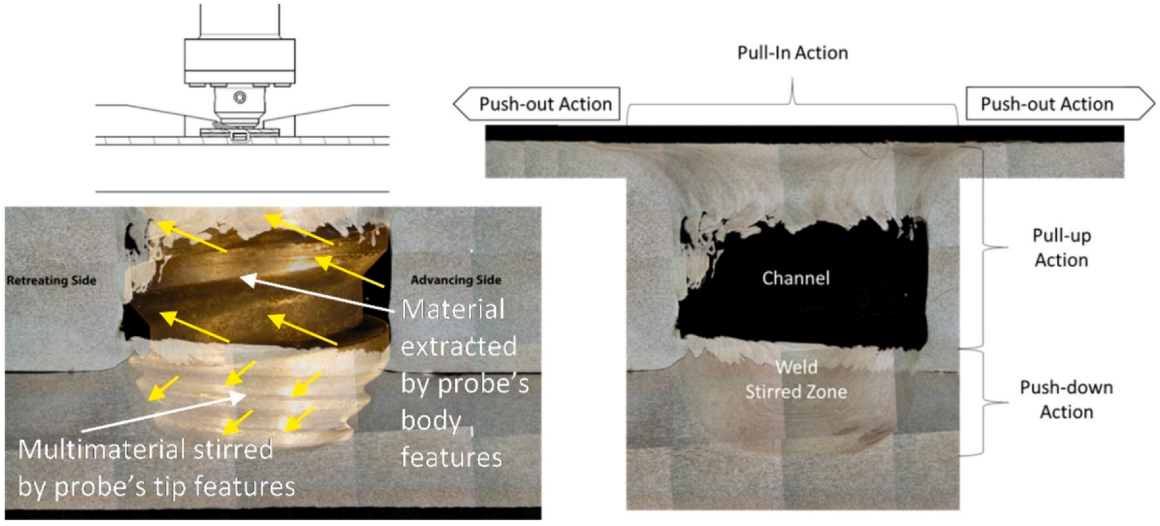

Fig. 1. Schematic representation of the fundaments of the hybrid friction stir channeling (HC) with simultaneous activation of the channeling and welding domains, emphasizing the interaction between the tool and the multi-material system being processed. The representation on the right, includes information on the push-pull effects prescribed by the shoulder and probe geometric features on the viscoplastized material flowing within the thermomechanically processed zone.

its alloys, which penalizes the sustainable use of Cu-based structures, due to the inherent increased weight and cost of the components. However, the density and cost per unit volume of Cu is significantly higher compared to the Al. Thus, the combination of Al-Cu based multi-material components, quasi-free of interfacial thermal resistance, enables optimal design of thermal management systems. For instance, the application of a lightweight thick Al rib containing a sub-surface channel along with solid-state welded thin Cu plate below Al rib. This provides an efficient thermal management of the targeted/external energy system through Cu thin plate and channel at Al rib with negligible interfacial thermal contact resistance, due to the physical continuity provided by the weld between the components. Besides, it is known that the fusion welding of Cu and Al is challenging due to dissimilar physical properties [12,13], such as fusion temperature, thermal conductivity and oxide layers, but also results often in brittle joints with reduced strength due to formation of defects [14,15], large intermetallic compounds (IMCs) [16,17], which in turn further deteriorate the mechanical properties [18,19]. This is addressed by HC as processing of Al-Cu system is in solid state processing by HC, which is similar like Al-Cu FSW [20] and Friction stir spot welding [21], and hence that overcomes the difficulties of fusion welding of Cu and Al.

As prior art to HC, the FSC was introduced as a manufacturing technique of internally closed channels in a monolithic plate. The FSC was originally introduced as an extension of the void defect that can be found in case of Friction Stir Welding (FSW) and Friction Stir Processing (FSP) [22], applied with incorrect parameters [23]. In the original concept of FSC, the extracted material was deposited in the clearance between tool shoulder and workpiece [24,25]. With this approach, if the clearance is too big, the channel is difficult to close, and for small clearance, the channel size is then very limited [26]. Meanwhile, the FSC underwent improvements of the technique, mostly via dedicated tool design, enabling to overcome the restricted the applicability of original concept and becoming a mature manufacturing process to produce subsurface channels in a wide range of sizes and shapes. Modern FSC, enables self-detachable flash concept without using clearance between tool shoulder and workpiece [27,28]. Different Al alloys AA1050, AA5083, AA5754, AA6082, AA6061 and AA7178 are investigated for processing of channel using different friction stir based channeling techniques, such as, FSC without the shoulder-workpiece clearance [29–31], stationary shoulder FSC [32,33], and HC [1,2], wherein the focus of the investigations is on single component or multicomponent system with same material. However, multi-material system with dissimilar materials, such as Al-Cu, is not investigated with channeling, despite the great potential of its applicability for demanding engineering applications like thermal management. There is a need to provide a solution with multi-material Al-Cu structurally stiff component with embedded conformal cooling channels suitable for thermal management application, so that substantial benefits such as lightweight structure, thermally efficient channels, cost effective manufacturing, reliable and robust solutions for thermal management of the ultimate high-power density (power/mass) systems can be obtained. Hence, the HC process, being a novel channeling solution, is specially dedicated for multi-material component system addressed hereon as Al-Cu multi-material system.

This paper presents the investigation on the application of the HC to an Al-Cu multi-material system with the stirring zone containing a large sub-surface channel, in the AA5083-H111, and a weld joint between the AA5083-H111 and the Cu-OF material components. The characterization of this multi-material system manufactured with HC assesses the channel's dimensions and all-around surface finishing of the sub-surface channel, microhardness map of the processed zone, and an in-depth analysis of the microstructural features of both channel and weld joint.

Materials and methods

In this investigation, HC was conducted considering following process principle, and analyzed its implemented for Al-Cu multi-material processing. In HC, the probe produces the stirring action in two different directions, which in turn results in pull-up action responsible for channel formation and pull-down action results in weld formation as can be seen from Fig. 1. The extracted material from probe's pull-up action, forming the sub-surface channel, is not deposited on the top surface of components, unlike in conventional FSC, but flows out of the processed domain by shoulder's features, being released as self-detachable flash, and hence flat surface is produced [1,2]. In the vicinity, of the shoulder's horizontal plane of action, the pull-in and push-out actions induced by the shoulder's features are responsible for forming the ceiling of the sub-surface channel, as can it is depicted in Fig. 1.

The application of the HC process for multi-material AA5083-Cu-OF system is conceptually represented in Fig. 2. Fig. 2(a) shows an Al

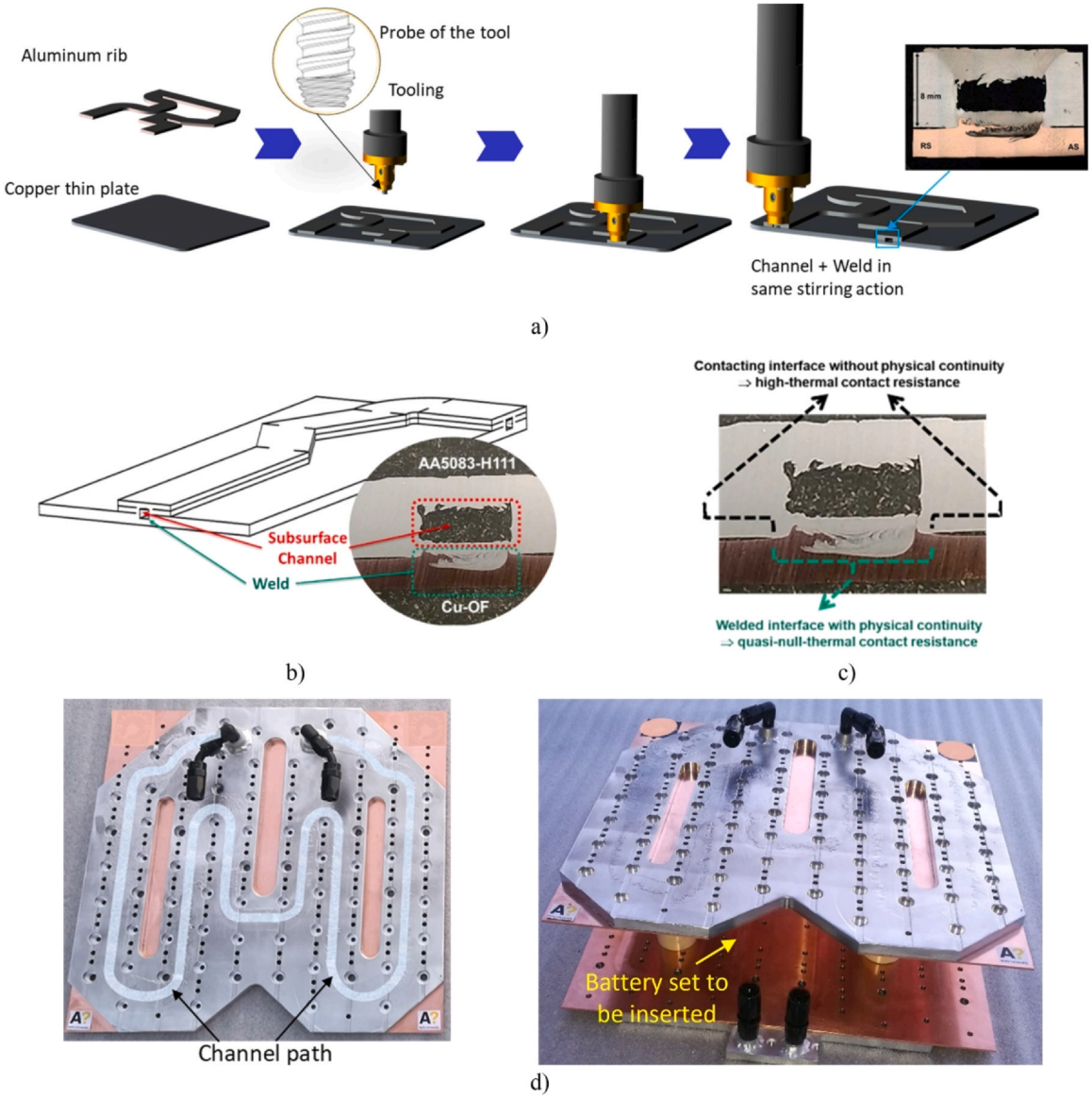

Fig. 2. Representation of the concept and application of the Hybrid friction stir Channeling (HC): (a) HC in the manufacturing of an Al-Cu multi-material system (Al rib over Cu plate), along a complex free-path, (b) and (c) simultaneous welding and channeling by HC, resulting in collecting all benefits from channeling while enabling material optimization with physical continuity, (d) implementation of HC to an Al-Cu multi-material system (AA5083 rib extracted from plate with 8 mm in thickness, and 3 mm thick Cu-OF plates with size 500 mm × 500 mm) applied in the thermal management of battery pack for electrical vehicles, wherein the battery set is to be inserted in-between the top and bottom components.

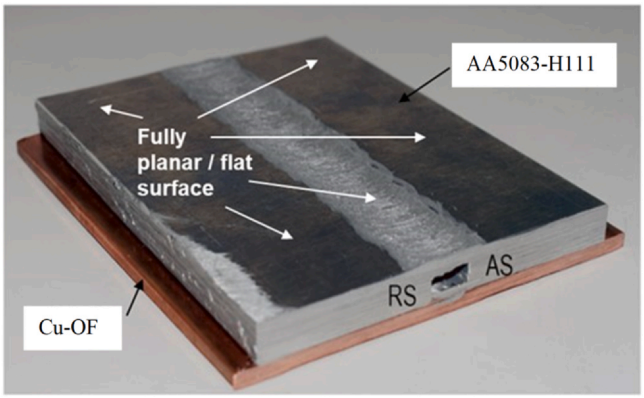

Fig. 3. Specimen in HC as-processed condition (no post-HC cleaning or machining). The AS, and RS, represent the advancing side (or shear side) and retreating side (or flow side), respectively.

rib with complex 2D path over a Cu thin plate to make Al-Cu multi-material structural system. This could correspond to the situation where the free surface of the thin Cu plate is applied in direct thermal management of a high-power source system, and the thick Al rib containing the channel, with a quasi-zero thermal resistance at the interface with the Cu plate (inherent to the welded interface), produces the thermal management of the Cu plate. With this combined approach it is possible to minimize the weight and cost (inherent to the Cu component), while providing the high-thermal performance of Cu, namely with fast answer to transient regimes and minimizing temperature differences between the hot and cold spots. A real implementation with the same technological conditions (tooling, HC parameters and materials) as the ones investigated in this paper is presented in Fig. 2(b)–(d).

The representative specimen selected to be investigated in this paper is the sample of Al-Cu multi-material system manufactured by HC, as represented in Fig. 3. The specimen is a stringer HC processing with about 160 mm in length. The HC was implemented on a multi-

Table 1
Typical chemical composition in %, of the AA5083-H111 alloy [34] and Cu-OF (½-hard) [36].

Alloying element	AA5083 in %	Cu-OF (½-hard) in %
Manganese (Mn)	0.40 – 1.00	-
Iron (Fe)	0.40 typical	-
Copper (Cu)	0.10 typical	99.95
Magnesium (Mg)	4.00 – 4.90	-
Silicon (Si)	0.40 typical	-
Zinc (Zn)	0.25 typical	-
Chromium (Cr)	0.05 – 0.25	-
Titanium (Ti)	0.15 typical	-
Aluminum (Al)	Balance	-
Bismuth (Bi)	-	Max 0.0005
Lead (Pb)	-	Max 0.005
Other elements		0.03

Table 2
Thermo-physical properties of the AA5083-H111 alloy [34,35] and Cu-OF (½-hard) [36,37].

Property	AA5083-H111	Cu-OF (½-hard)
Density [kg/m^3]	2650	9000
Thermal conductivity [W/m/K]	121	390
Melting temperature [°C]	570	1080
Coefficient of thermal expansion [1/K]	$25{\cdot}10^{-6}$	$17{\cdot}10^{-6}$
Specific heat at 20 °C [J/(Kg*K)]	900	419

material system of 8 mm thick AA5083-H111 and 3 mm thick Cu-OF (½-hard) in overlapping joint configuration, keeping the Al alloy in contact with the tool shoulder, and the Cu in contact with the anvil. Chemical composition and thermo-physcial properties of AA5083-H111 [ThyssenKrupp, Springer Handbook of Materials] [34,35] and Cu-OF (½-hard) [36,37] [MetalCenter, Heat transfer handbook] are shown in Table 1 and Table 2. Specially designed HC tool, consisting of a 10 mm in length probe with 10 mm in diameter, and a 22 mm in diameter scrolled shoulder.

An ESAB Legio FSW 5UT machine was used in HC-based manufacturing of the test specimen. The Table 3 presents the processing parameters used for the HC. This set of parameters are considered based on the results from numerous laboratorial experiences and best procedures in reaching stable, defect-free, and repeatable results, with HC of these materials and geometry.

The processed HC sample was subjected to visual examination, cross-sectional macrostructure analysis, optical 3D scanning of channel surfaces, optical microscopy (OM) and scanning electron microscopy (SEM), energy dispersive X-ray spectroscopy (EDX), electron backscatter diffraction (EBSD) and micro-hardness measurement. The band saw and the circular saw machines were utilized for extraction of specimen to perform the cross-section-based analysis. The geometrical features of the channel's surfaces were investigated by SEM and optical 3D scanning. The samples were sliced by wire cut electro-discharge machining from the center of the channel along the longitudinal direction, in order to have open access to the top and bottom surfaces for imaging and scanning. The optical 3D scanning was performed after applying a thin layer of matt grey paint on the surfaces to avoid reflections, using a scanner, based on blue light to project fringe patterns that are captured by two cameras, in an incremental step of 23 mm.

The microscopy was performed after standard grinding procedure followed by polishing on 1 µm diamond paste and 30 s swabbing of etchant (15 ml HF + 10 ml H_3PO_4 + 60 ml water) on the Al side. High magnification camera was used to capture the OM images. SEM and EDX were carried out with a compact electron microscope. The cross-sectional specimen was further grinded and polished with 0.25 µm abrasive paste using mechanical grinding and vibro-polishing, to characterize SEM-EDX and EBSD.

The indentations for microhardness were performed at 1 mm interval with a load of 500 g on the cross-section of the processed specimen using a micro-combi tester. Force-displacement curves of Oliver and Phar method [38] were used to measure the HV(IT)05 microhardness.

Results and discussion

Visual analysis and macrostructure

The application of the HC process to the multi-material system composed by the thick plate of AA5083-H111 and thin plate of Cu-OF is depicted in Fig. 2. The extracted specimen, in HC as-processed condition, is presented in Fig. 3. From the visual analysis of the top surface of the specimen, it is possible to confirm that the top surface, directly in contact with the shoulder, is flat and do not exhibit any left-over flash. This is an advantage of manufacturing as no step effect is resulted and hence the problem of material deposition at clearance between shoulder and workpiece in conventional FSC as noticed in [24,25] is solved in present investigation by HC with fully planar and flat surface. In HC, all the extracted material, from the Al component, is detached in form of self-detachable flash, keeping zero gap between the shoulder and the processed materials.

The Fig. 4 shows the typical cross-section of the Al-Cu HC processed sample. A large quasi-rectangular shaped channel, and a weld, co-exist in the same stirred zone, without any visually detectable defect was obtained. An average channel's width of 9.6 mm, and channel's height of 3.3 mm, fully located within the Al domain of the stirred zone, are obtained. These channel dimensions are the larger obtained when compared to previous literature [23–25,39–41]. Differently from other authors approaches, these large dimensions of the channel produced by HC, are enabled by the synchronized pull-up effect induced by the probe action of material extraction, on the mass of Al component, and the push-out effect into external self-detachable flash at the same flow rate of mass of Al material induced by the shoulder action. This synchronized effect, corresponding to the mechanisms of channel formation with HC, was schematically represented in Fig. 1. Besides, the stirring-mixing action underneath of the channel is responsible for the welding of the overlapping joint Al-Cu. The features of this welding zone are mostly created by the probe's tip domain of the tool. From Fig. 4, it is possible to notice that the defect free weld joint of dissimilar materials, does not affect the stable formation of the large rectangular channel.

The Fig. 4 depicts distinct surface features at the walls of channel namely the ceiling side, flow side (RS), shear side (AS), and the bottom side that stands over the weld zone [3]. The shear side (AS), and the bottom side, act as well-defined origin walls of channel, mostly prescribed by the tool geometry. Emphasis for the fact that differently from the FSC of [23–25,39–41], the bottom surface of the channel is not defined by the tip of the probe, as the probe is longer than the Al thickness, and plunges deeper into the Al-Cu joint in HC. The flow side (RS), and ceiling wall act as channel closing surfaces, defining the shape and stability of the channel. The material shears

Table 3
Processing parameters used in the HC of the multi-material system composed by the AA5083-H111 and Cu-OF and represented in Fig. 3.

Travel speed [mm/min]	Rotation speed [rpm]	Control mode	Dwell time [s]	Tilt angle [°]	Shoulder-workpiece clearance [mm]
90	300	Position control	2	0	0

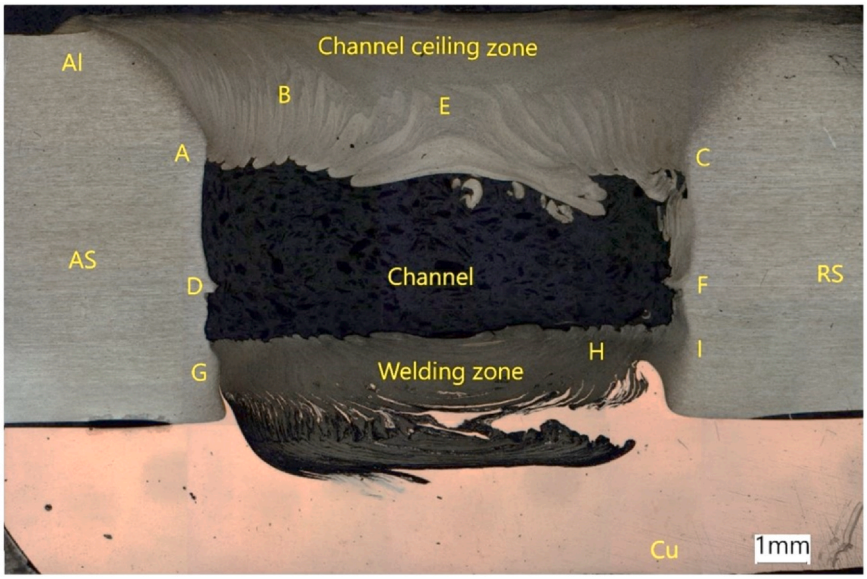

Fig. 4. Macrograph of the cross-section of specimen presented in Fig. 3, resulting from the HC of the Al-Cu multi-material system. The AS, and RS, represent the advancing side (or shear side) and retreating side (or flow side), respectively.

from AS and extracted through pull up action led to closing sides at RS and pull out from shoulder led to ceiling wall of channel. Therefore, closing sides of flow side (RS) and ceiling side define shape and finishing of channel by the HC processing parameters. Quantified analysis on channel surface's finishing is presented in following sub-section.

Surface Profiles of Channel

Figs. 5 and 6 show surface features of the channel by optical 3D scanning and SEM, respectively. Roughest surfaces of channel are observed at the ceiling side, as can be seen from Figs. 5(b) and 6(b), and surface towards flow side (RS), as can be seen from Figs. 5(b) and 6(a), (b) and (d). Since these surfaces are formed due to closing of channel, the deposition of extracted material at ceiling side and leftover unextracted material at retreating side during processing create rough surfaces on ceiling side and flow side (RS). Besides, the shear side (AS) surface presents the smoothest finishing due to the shear origin, as can be seen from Fig. 6(c), as compared to rest of the other surfaces in Fig. 6. The bottom surface of the channel has an intermediate value with regular scrolled striates distribution from 300 µm to 450 µm. These stirring ripples of geometrical regular features at the bottom surface of the channel remain uniform because they are mostly induced by the processing pitch ratio [300 µm/rotation], i.e., ratio of travel speed [90 mm/min] versus spindle rotation [300 rpm], that remains the same throughout the length of the HC processing. The ceiling zone of the channel was created due to combined action of the rotating shoulder travelling over the top surface of the Al rib, and top part of the travelling-rotating probe, plunged in the Al-Cu multi-material system. Where the top part of the tool's probe forges the material against the shoulder, and the tool's shoulder extracts the part of Al material into detachable flash while forges the remaining part of Al material below the shoulder. This in turn closes the channel with an irregular surface finishing, that increases towards the flow side (RS) where the roughness values range from 720 µm to 1600 µm at zone 1 of Fig. 5(b), versus about 500 µm at zone 2 of Fig. 5(b). These irregular features of channel's surface finishing, provide an extraordinary benefit for thermal management, as it was demonstrated by Karvinen et al. [11] with about 45 % better heat transfer rate as compared to same shape and dimensions of smother channel fabricated by conventional milling operation. Although outside of the scope of the present paper, it is worth to correlate current results of surface roughness obtained on channels' wall surfaces for heat transfer improvements using the channels from FSC [11] or HC [2], should be due to promotion of large layer of turbulent fluid flow, even for small flow rates, and increased surface area of the internal walls of the channels, for the same overall shape and size.

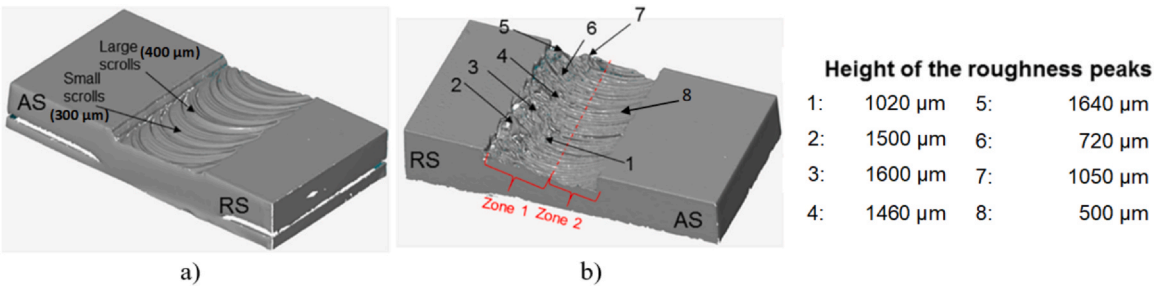

Fig. 5. Channel surface profiles after 3D optical scanning: (a) bottom surface, and (b) ceiling surface.

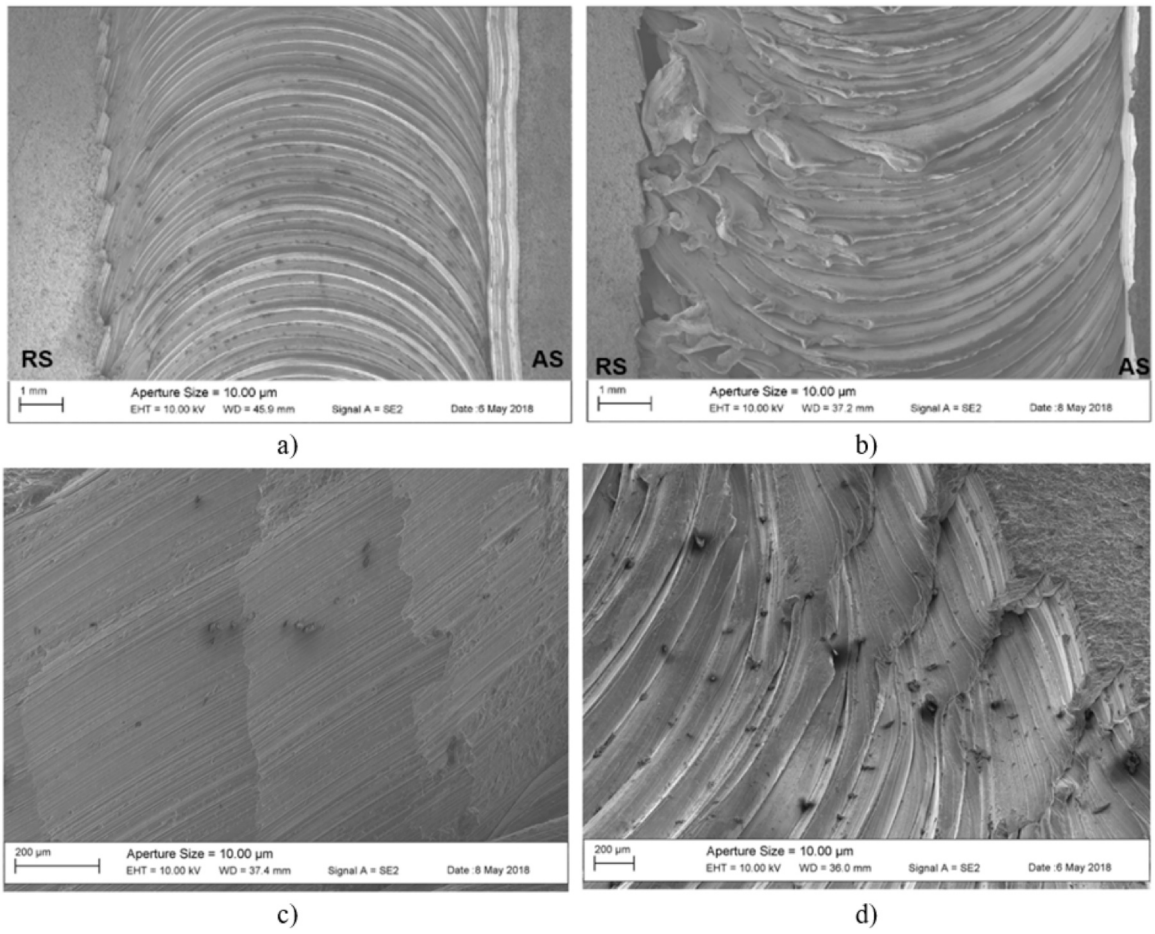

Fig. 6. – Scanning electron microscopic (SEM) images of channel surfaces: (a) bottom surface, (b) ceiling surface, (c) Shear side (or advancing side, AS) wall, near top surface, and (d) corner of channel between bottom and flow side (or retreating side, RS) surfaces.

Microhardness measurements

Microhardness measurements are carried out, covering the Al alloy and Cu base materials (BM), and the processed domains, namely the thermo-mechanically affected zone (TMAZ), and the heat-affected zone (HAZ). The TMAZ encompasses the stirred zone (SZ), where the bulk viscoplastic deformation, and inherent heat dissipation, result in dynamic recrystallization, as previously reported by [42], on research of friction stir-based processing techniques. In the present investigation, the channel and weld domains are formed within the SZ, and hence they are possibly surrounded by TMAZ and HAZ.

Fig. 7 depicts large variations of hardness, from 65 HV(IT) 05–329 HV(IT)05, measured within the cross-section of the processed domain of the specimen extracted from the Al-Cu multi-material system presented in Fig. 3. The highest hardness peak is noticed at the Al-Cu weld zone, and lowest harnesses are measured in the TMAZ, of both the AS and RS of the channel. Additionally, the weld zone is observed with large hardness variations, from 100 HV (IT)05–329 HV(IT)05. This has occurred as this zone contains complex phases like solid solutions of Al and Cu along with IMCs, namely having Cu rich lamellae zones, specific phases of Al-Cu IMCs, and Al matrix, and all these phases consist of different hardness variations. These variations of hardness in the weld zone confirm metal matrix type composite structure with heterogeneous distribution of Cu lamellae and IMCs in Al matrix. It can be correlated from Fig. 8 that the indentation sizes are different at Cu side, Al side and layered structure at the interface region, including indentation on the IMCs. The differences in indentation sizes after the hardness measurement done, confirm that the weld zone has heterogeneous behavior in hardness, and that is because of various phases are presented within this zone. Smallest hardness indentation is observed in Fig. 8(b), for the hardness measurement of 329 HV(IT)05, wherein the hard and brittle nature of IMCs has resulted to high hardness as compared to Al and Cu materials. Later in this paper, the elemental analysis is investigated on this location to identify the possibility of having specific formation of IMCs at this location, and to correlate the hardness measurement for this location. Besides, the lower hardness measurements are mostly found at channel's surrounding (i.e., at the surfaces of channel), which is because the forging consolidation effect on the Al material is absent due to no pressure.

The hardness measurements of the ceiling zone show variations in between 80 HV(IT)05–100 HV(IT)05. These hardness values are slightly higher than the Al base material. The higher hardness at the channel's ceiling, mostly located at the AS of the ceiling, will provide enhanced strength and mechanical resistance to high-internal pressure loading of the channel. The AS of the channel's ceiling is a region experiencing discontinuous dynamic recrystallization as compared to the one at the center of ceiling zone, because this is the region where the final closing of the sub-surface channel is formed. These variations in the hardness maps are attributed to the microstructural evaluations of finer grain structure due to continuous/discontinuous dynamic recrystallization and may be due to Hall-Petch strengthening mechanism at these specific locations., This can be correlated from Fig. 9(a) and (c) as an example where fine grain microstructures were noticed at stirred regions.

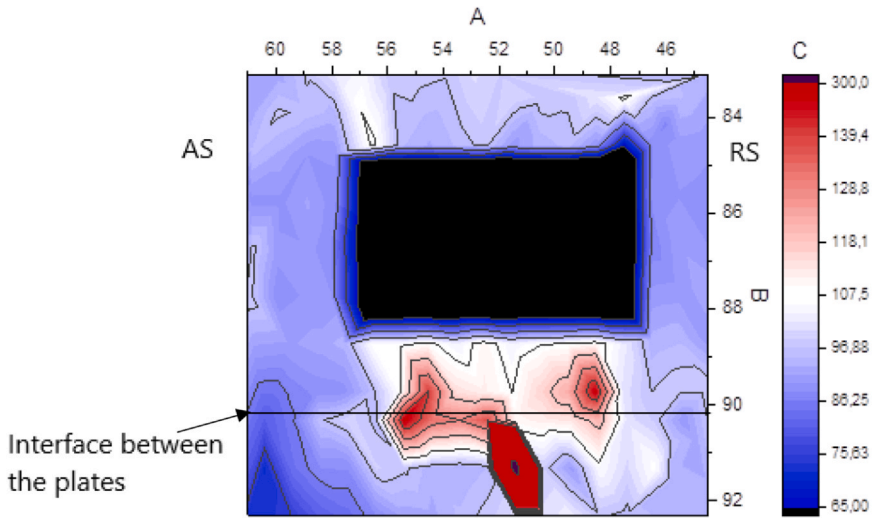

Fig. 7. Microhardness field with indentation force of 500 g (using Oliver and Pharr method) HV(IT)05, of the processed domain of specimen presented in Fig. 3, resulting from the HC of the Al-Cu multi-material system.

Microstructural characterization with focus on the channel domain

The microstructural features of the cross-section of the HC specimen are depicted in Fig. 9. The SZ encompasses the channel and weld domains with distinct microstructural features among them, and around these processed regions. Surrounding the SZ, microscopically distinct zones are the TMAZ, the heat-affected zone HAZ and the unaffected Al alloy and Cu base materials. The Fig. 9(a) and (b) depict the interface between the stirred zone and the TMAZ At the AS of the channel's ceiling zone. The emphasis here is on the progressive consolidation of channel, closing at the shear side and layered resulting from effect of tool's movement and stirring effects. Namely, the joining consolidation is achieved via the effect of the upper part probe's features in the flow of the Al material against the shoulder. The shoulder features are then responsible for the extraction of the Al material into detachable flash, enabling the formation of the large sub-surface channel via forging the remaining Al material forming and quasi-uniform ceiling zone. At the top zone of this interface, the Al material is forged against the sheared surface under the influence of the shoulder, and thus under high forging force, the bottom part of this interface is forged like in open die conditions, because of the empty channel domain, and so the atomic bonding and diffusion joining mechanisms in solid-state welding are not fully consolidated, resulting in a small extension of unbonded region at the channel's corner of AS-ceiling zone interface as can be seen from Fig. 9(b). The relation between the length of this unbonded interface and the thickness of the ceiling layer closing the channel, is one critical issue, acting as fracture initiation and governing the fracture propagation and localized corrosion phenomena that will control the performance of the FSC and HC components, as it was confirmed in bending [43], torsion [44], fatigue loading [45] and internal pressure tests [46].

All this severe plastic deformation and large-scale stirring material flow effects, results in dynamic recrystallization leading to a refined grain structure, noticeable in all the stirred zone, with emphasis for the domains with exclusive Al material. Distinction of grain refinement between the unstirred and stirred zones can observed in Fig. 9(a), (c), (d) and (f), wherein it is possible to see great level of grain refinement. The microstructure regions adjacent to the channel are influenced from the combined tool's travel plus rotative motions, resulting in distinct AS and RS, as can be depicted from Fig. 9(d) and (f), respectively. At the middle zone of the channel, the TMAZ at the AS includes only a narrow layer of stirred material, less than 100 μm in-width, when compared to the TMAZ at the RS, that contains a significant layer of SZ, reaching an average of about 400 μm in-width. These differences are inherent to the material flow

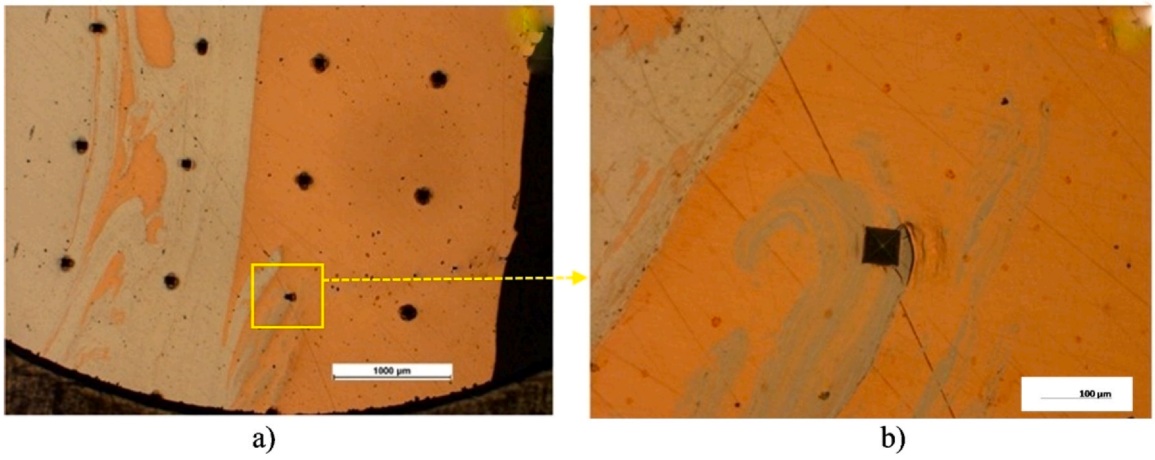

Fig. 8. Detail of microhardness indentations: (a) at Al-Cu interface, and (b) at intermetallic compound with hardness peak of 329 HV(IT)05.

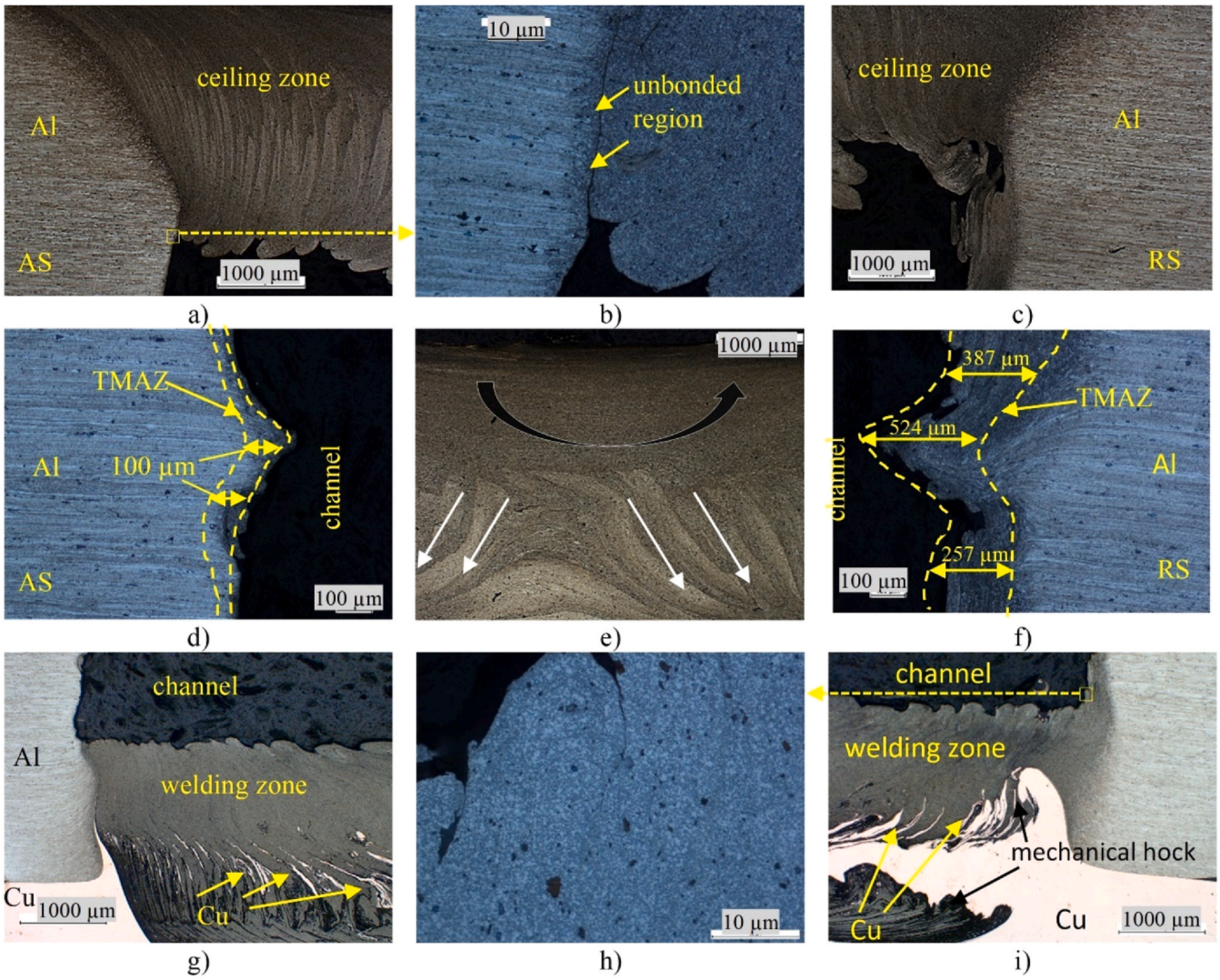

Fig. 9. Optical microscopy images surrounding the channel and weld regions: (a) advancing side (AS) of channel ceiling zone, (b) unbonded interface between ceiling zone and non-stirred Al material for location shown in image (a), (c) retreating side (RS) of channel ceiling zone, (d) shear side (or retreating side, RS) of channel's middle zone, (e) material flow and forging features mostly influenced by shoulder action at channel ceiling layer, (f) flow side (or retreating side, RS) of channel's middle zone, (g) AS of the weld zone between Al-Cu interface, (h) detail of channel's corner with weld zone at RS, and (i) RS of weld zone between Al-Cu interface; Locations of (a) to (i) are shown in Fig. 4 as (A) to (I).

with channel formation. Since the extraction of material originates from shearing action at the AS, with transport of material towards the shoulder and through the RS, where mechanically deformed material loses momentum, and is deposited. Thus, differently from the well-known material flow in the FSW process, in HC the Al material does not flow around the probe, preventing to fill the empty trailing side of the probe, and enabling the formation of the sub-surface channel.

Partially recrystallized grains are predicted in both TMAZs as they are affected by mechanical deformation and thermal effects. This is confirmed later through EBSD analysis. Also, no distinct HAZ is noticed with microstructural variations, at either side of the channel and weld zones, unlike in FSW process. This is due to the heat input during HC to be lower than in FSW. This fact results from the significant amount of energy continuously extracted from the processed zone, in the form of flash. This flash is in viscoplastic domain, and therefore a very hot mass, of Al material.

The microstructures within the processed region below the channel, with Al-Cu materials mixing is depicted in Fig. 9(g) and (i). The defect free welding is established in this zone, The dispersion of Cu mixed in Al matrix will be analyzed in next section.

Microstructural characterization with focus on the Al-Cu weld domain

The welding between the Al-Cu components in overlap configuration is positioned just below the channel, as presented in Fig. 9(g) and (i). The weld region towards the RS shows mechanical hooking effect of Cu in Al matrix, whereas no such hook formation observed towards the AS of the weld region but noticed with sharp edge of Cu at the corner of weld zone's advancing side. The shear originating action mentioned in channel formation is similarly observed as driving phenomenon for such feature, where origin of shear at AS resulted to fine dispersion of Cu lamellae within Al matrix, while at RS resulted in thick Cu lamellae and Cu's hooking in Al matrix.

The grain refinement of weld zone region can be confirmed from EBSD images presented in Fig. 10. The stirring action imposed by the HC tool, in the thermomechanical processed zone of the based materials, promotes high localized straining effect and raised temperature of material mostly due to bulk plastic deformation with contribution from frictional heat. At high strain and temperature above recrystallization temperature, the grain size decreases significantly due to continuous dynamic recrystallization. Therefore, ultrafine grains are observed in the stirred zone region as compared

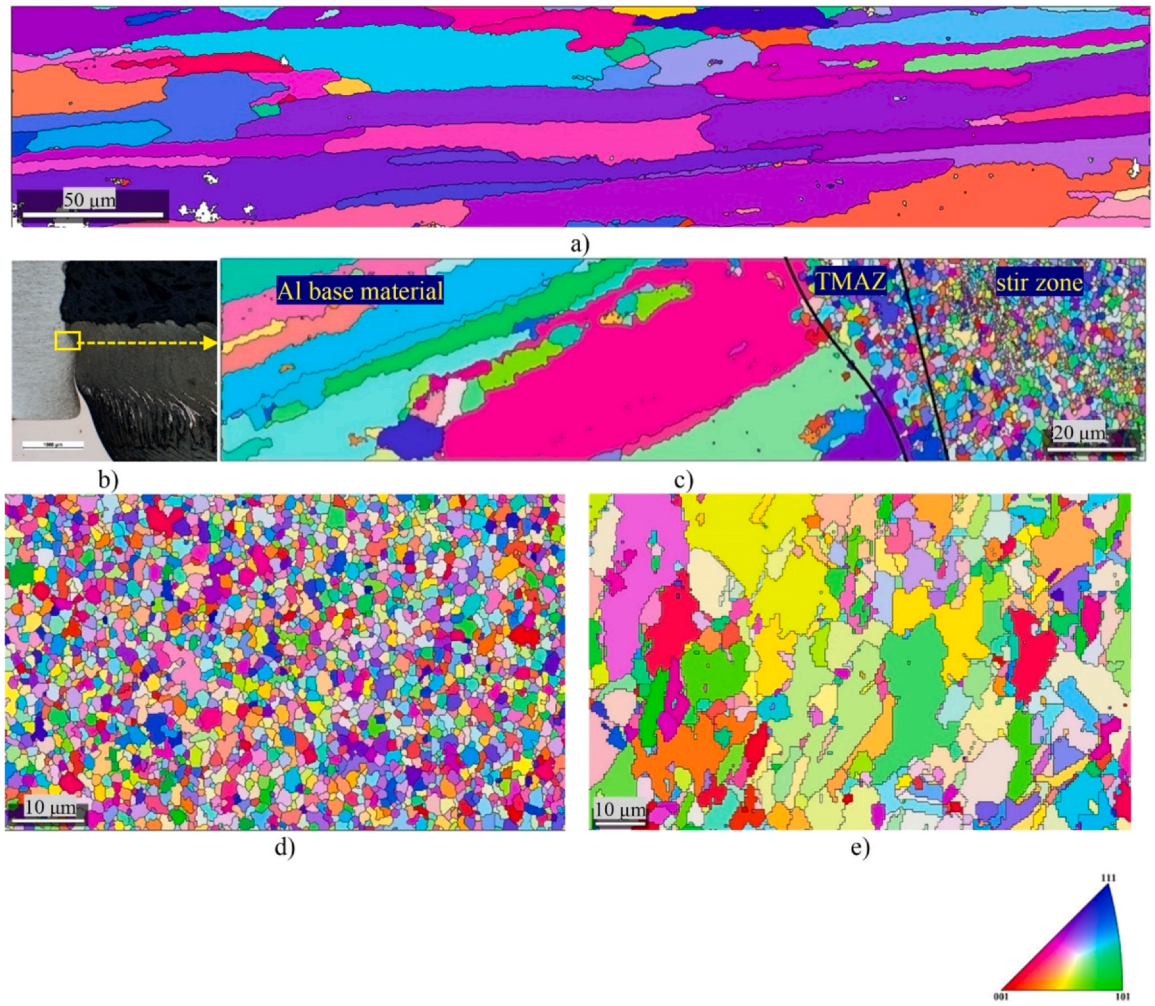

Fig. 10. Images *from e*lectron backscatter diffraction (EBSD) showing grain *structure and texture at both base materials and within the processed zone*: (a) AA5083-H111 base material, (b) reference macro image showing location for EBSD analysis, (c) weld zone-Al matrix interface for location shown in image (b), (d) stirred zone of the TMAZ, and (e) Cu-OF base material.

to the base material regions. The refined grains can be found within the whole TMAZ, including the stirred zone.

The typical microstructure for rolled plates of AA5083 is observed, with elongated grains in the direction of rolling, with 42 µm mean grain diameter and 290 µm^2 mean grain area, as depicted in Fig. 10 (a). In case of microstructure of the Cu-OF base material, it is observed grains with parallel straight-lines (referred as twins, and typical from annealed Cu-OF), with 5.1 µm mean grain diameter and 13.2 µm^2 mean grain area, as shown in Fig. 10 (b). In the Al matrix, at the weld zone, it is observed ultra-fine equiaxed grains, with 1.9 µm mean grain diameter and 1.7 µm^2 mean grain area, as presented in Fig. 10 (c) and (d).

The great level of refinement is only noticeable in the Al material. Whereas the Cu experiencing bulk deformation does not undergo significant grain refinement, and that, in turn, resulted to Cu fragmentation. These fragments of Cu are shaped into thin lamellae structure, and are mixed, or intercalated, in the Al matrix of the Al-Cu weld domain, as can be seen from Fig. 11. There is no evidence of defects observed in the weld zone, with most of the complex intermixing between the Cu lamellae and the Al matrix, exhibiting a good consolidation of the joining mechanism, mostly via solid state interdiffusion between Cu and the Al. The fragmentation of Cu can be observed as non-planar layered type of structure with different thicknesses and lengths. Ultra-fined microstructure is observed at top region of weld zone where Al is present, without presence of Cu. The Cu lamellae is found mostly at the bottom of the weld zone due to dispersion of Cu material under the forging with shear and stirring actions by probe shape and features responsible for the resulting microstructure at the weld zone. These lamellae are moved through stirring action, and eventually mixed with Al matrix where interatomic diffusion is obtained under the action of heat induced by plastic deformation and friction, along with forging pressure caused by features of the probe. The previous literature also claim that the metal matrix composite type structure and/or mechanical interlocking provide defect free dissimilar FSW joints [46–48].

To further evaluate the consolidation of the joining between Al-Cu, SEM images are presented in Fig. 12. It is possible to notice that along with a general strong joint consolidation, there are few interfaces with poor joint consolidation. The poorly consolidated interfaces are mostly outside of probe's interaction in Al-Cu materials. In the stirred zone, the contact of probe with Cu material resulted to fine lamellae intercalated with Al material. In this region, most of the heat is generated through bulk viscoplastic deformation and that is enough to activate strong joining consolidation between Al-Cu materials within the stirred zone. At the interface of TMAZ with base material, it is possible to notice different levels of joining consolidation, as can be seen from Fig. 12 (F) to (K). In general, outside of the SZ there is the trend to find some poor-consolidated zones

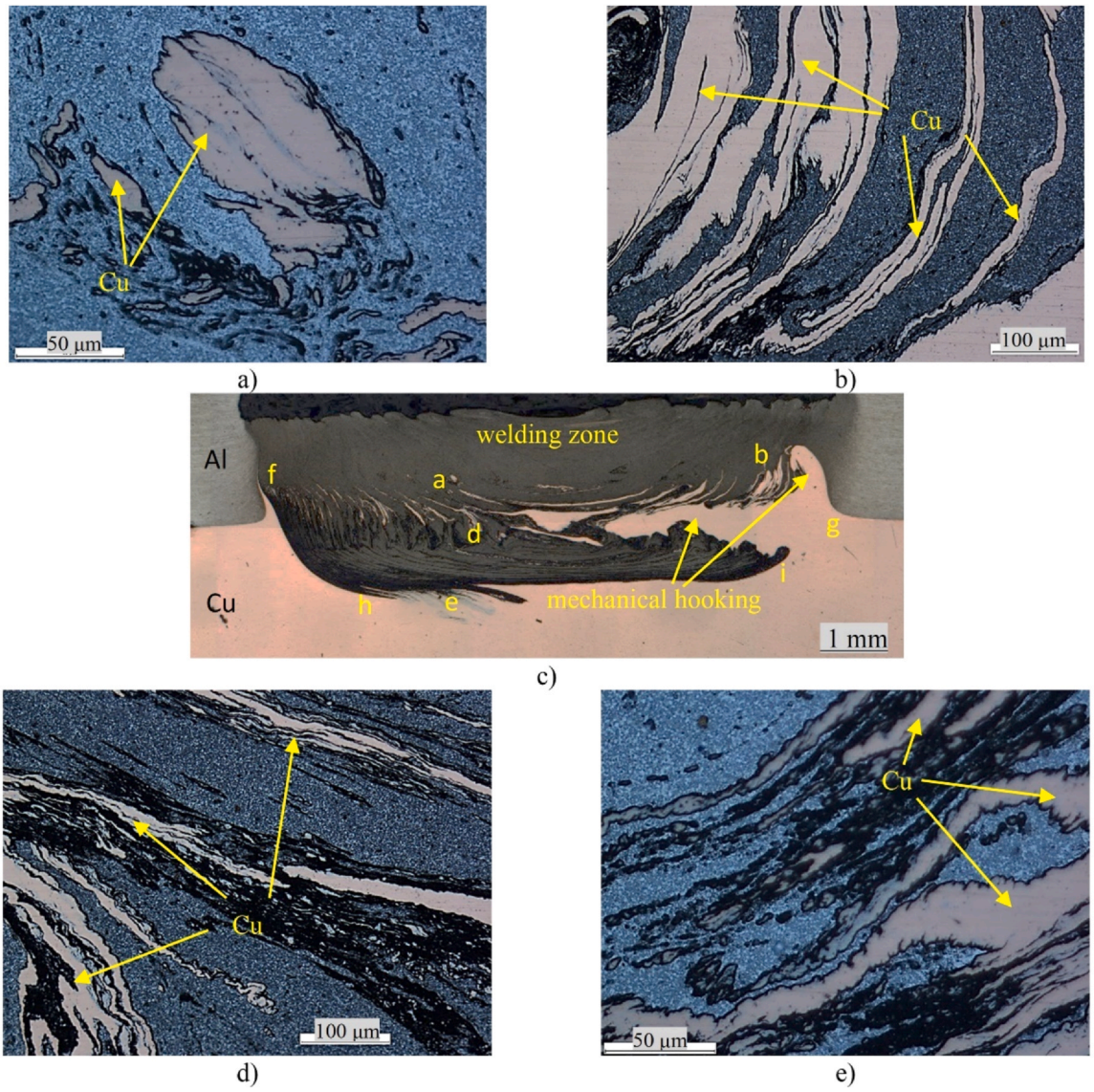

Fig. 11. Microstructural analysis of the Al-Cu welding domain: (a) location A in image (c), (b) location B in image (c), (c) macrograph with focus on welding zone and points of interest for microscopic analysis, (d) location D in image (c) and (e) location E in image (c).

around the Cu lamellae. But there is continuous metallurgical joining between Al-Cu in the SZ below the channel. This emphasizes how HC is suitable to apply in thermal management where strong metallurgical joining consolidation helps in high heat transfer efficiency, e.g. as compared to strongly clamped components vias mechanical joining [2].

The reaction layer of IMCs is identified at the interface (Fig. 12H and L) and around the Cu lamellae Fig. 12 (I) and (M). Fig. 10 (L) shows that the IMCs layer is as thin as 229 nm, which is positive in case of dissimilar welding, as recommended in literature [46,47,49]. In other locations between Al-Cu interface, the visual analysis from Fig. 12 can be made as there were no major variations observed in IMCs' thickness because of controlled low heat input conditioning caused by HC. This shows favorable low heat input conditions used in HC processing has helped to obtain IMCs' thin layer to control the solid state interdiffusion between Al and Cu materials, that in turn resulted to effective strong consolidation of the joint. The phase identification of IMCs is predicted by SEM-EDX analysis in the next section with elemental analysis.

Elemental analysis

The elemental analysis on Al-Cu interface, made at specific location of E from Fig. 11 (c), where maximum hardness values are observed, is carried out with spot and line mapping as shown in Fig. 13 and Fig. 14 respectively. The formation of IMCs and materials mixing between Al and Cu was obtained via by SEM-EDX with the results presented in Fig. 13, Fig. 14, and Fig. 15. Fig. 13 shows different locations from where different locations are selected for spot EDX analysis. Also, the selected region from same image as shown by rectangle in Fig. 13 is considered for line mapping by EDX to observe the continuous evolution of chemical composition and those results are presented in Fig. 14. It can be confirmed that the IMCs are likely to exist at around line mapping position 45 µm and 115 µm, where layered, or lamellae, structure is observed, as shown in Fig. 14. Therefore, variations in hardness are observed considering heterogeneous structure distributed in whole weld zone. This also, confirms that weld region has strong metallurgical consolidation, including IMCs formation.

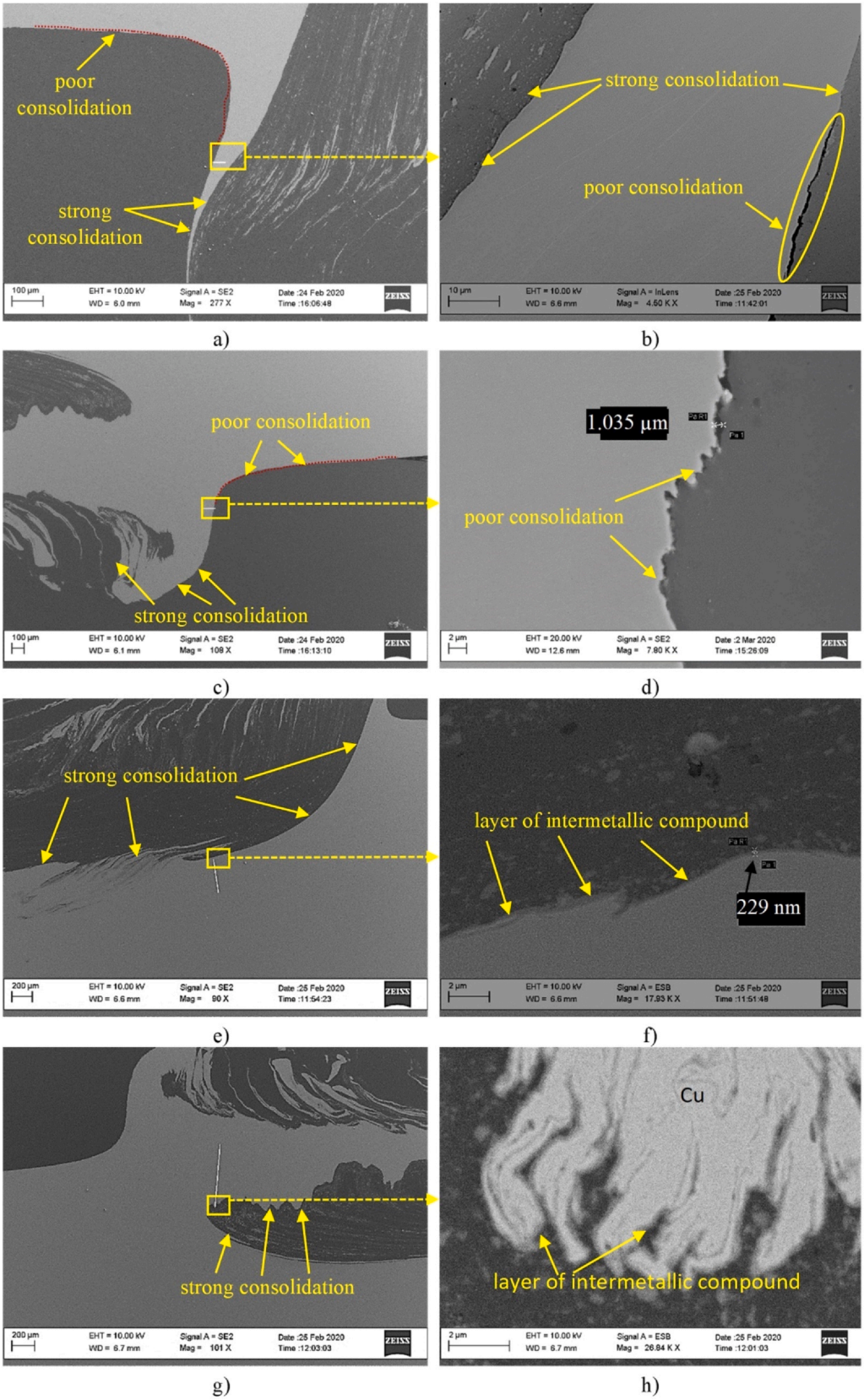

Fig. 12. Scanning electron microscopy images for stirred zone (SZ) at Al-Cu interface as identified in Fig. 11 (c): (F) advancing side, (J) higher magnification image of location J mentioned in image F, (G) retreating side, (K) higher magnification image of location K mentioned in image G, (H) bottom part at advancing side, (L) higher magnification image of location L mentioned in image H, (I) bottom part at retreating side, (M) higher magnification image of location M mentioned in image I.

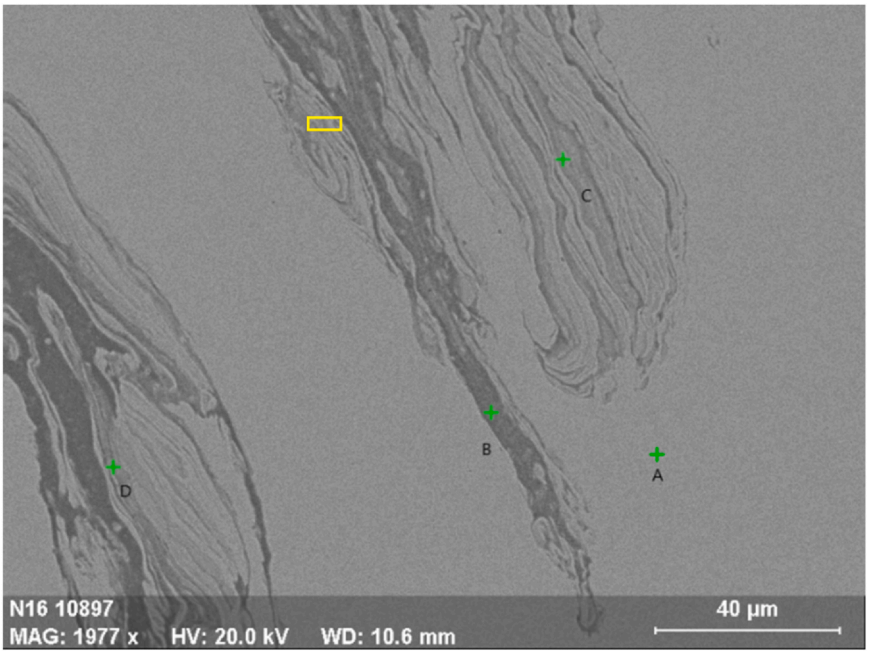

Fig. 13. SEM image showing spot locations of EDX analysis from the location E of Fig. 11 (c).

Fig. 15 and Table 4 show the results of spot EDX performed at points A, B, C and D, identified in Fig. 13. Using Al-Cu binary phase diagram [50], the presence of IMCs is identified and predicted. Location C has composition 43.66 % Cu and 52.51 % Al, and D has composition 45.79 % Cu and 50.90 % Al, refer Table 4. The presence of Cu, and Al, solid solution exists at location A (100 % Cu, refer Table 4) and B (13.82 % Cu, 82.65 % Al and 3.37 % Mg, refer Table 4). IMCs of Al_2Cu, Al_9Cu_4, and Al_2Cu_3 from Al-Cu binary phase diagram are not likely present due to low heat input inherent to the HC processing, wherein it is expected to have insufficient activation energy and low free Gibb's energy required to form abovementioned IMCs phases. Therefore, it is possible to confirm that the solid state inter diffusion between Al and Cu phases and activation energy for IMCs govern the formation of IMCs in case of HC between Al-Cu multi-material system. Additionally, in Table 4, Mg is also found along with Al-Cu that may be because this element, originally in solid solution of the AA5083 Al-alloy, is presented at the surrounding of respective IMCs phase and identified due to the placement of the spot has covered extra regions from the IMCs.

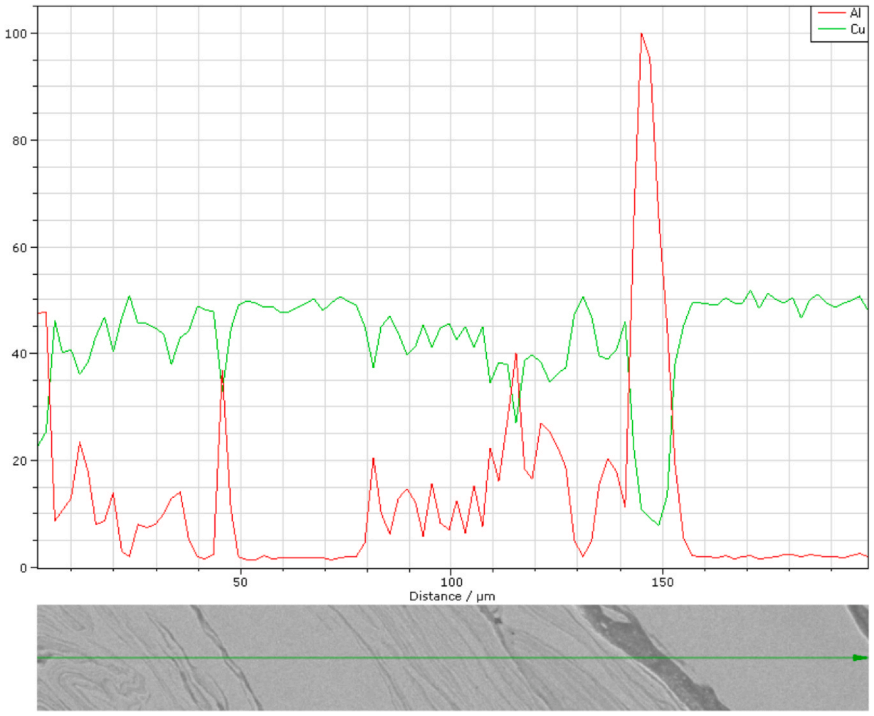

Fig. 14. Line EDX result from the area shown by rectangle in Fig. 13.

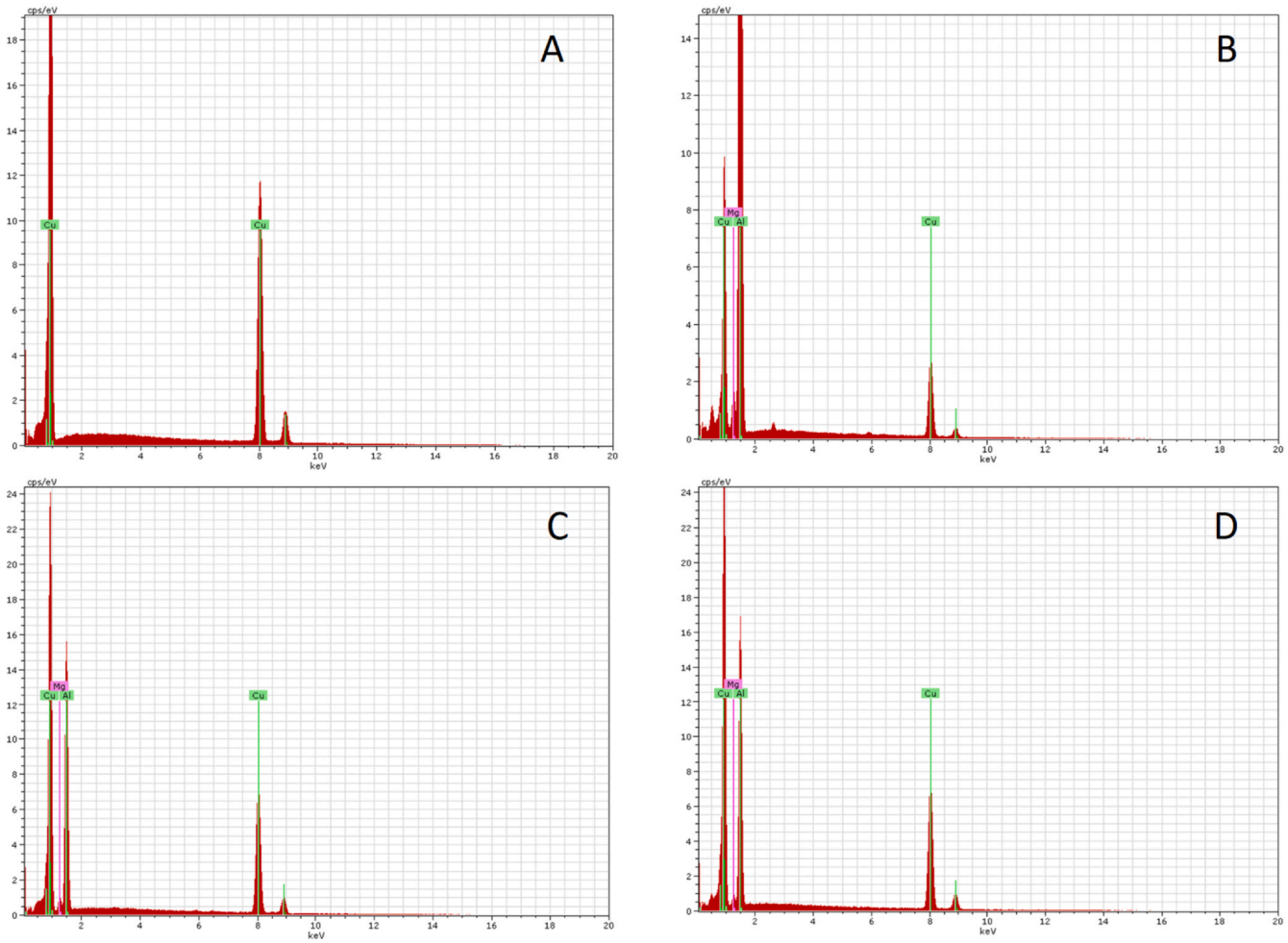

Fig. 15. EDX spectrums of indicated points in Fig. 13.

Table 4
Quantitative results of the EDX analysis for spot mentioned in Fig. 13.

Zone	Copper (Atomic %)	Aluminum (Atomic %)	Magnesium (Atomic %)	Interpretation
A	100	0	0	Copper
B	13.98	82.65	3.37	Al rich solid solution
C	43.66	52.51	3.82	AlCu + Mg
D	45.79	50.90	3.31	AlCu + Mg

Conclusions

In this investigation, novel manufacturing of multi-material Al-Cu system by hybrid friction stir channeling (HC) is presented and analyzed for processing influence on microstructure evolution and properties at around the processed zones. The investigation of the processing and metallurgical conditions of HC, brings forward the following conclusions:

- HC provides a solution to produce sub-surface channel completely on Al rib along with defect free welding to thin Cu plate just below the channel in single manufacturing action, where the produced channel's size is 9.6 mm in-width and 3.3 mm in-height, quasi-rectangular shape, and step-free effect on the processed top surface.
- The sub-surface channel produced by HC in Al rib component consists of unique wall surface features, with non-uniform and non-oriented surface roughness, suitable to activate turbulent fluid flow and therefore to enhance the efficiency in thermal management applications.
- The welding between Al-Cu components, obtained at just below the sub-surface channel, resulted in defect-free joints, with effective metallurgical consolidation via mechanical interlocking of Cu lamellae, or layers, stirred in the Al matrix. The continuous joining contains only short-length and thin intermetallic compounds (IMCs) at Al-Cu interface.
- Increased hardness is obtained at the IMCs locations, in the stirred region of weld joint, reaching a maximum microhardness of 329 HV(IT)05.
- High strength stirred domains are obtained in ceiling zone, with emphasis for the advancing side (AS), where higher microhardness as compared to base materials of Al and Cu are obtained. The ceiling zone is observed with intermediate hardness values in between 80 and 100 HV(IT)05.
- The effective potential of manufacturing multi-material component for applicability in thermal management system is demonstrated, and results features obtained from HC, are evaluated with support from published literature.

Declaration of Competing Interest

The authors declare that they have no known competing financial interests or personal relationships that could have appeared to influence the work reported in this paper.

References

[1] H. Karvinen, P. Vilaca, D. Nordal, A Non - Consumable Tool and a Process For Solid - State Production of a Channel and a Weld Joint, and a Structure of at Least Two Components Based on Originally Bulk Components of Similar, or Dissimilar, Materials, US 2019 / 0210147 A1, 2019.

[2] Karvinen, H., Nordal, D., Galkin, T., Vilaça, P., 2018, Application of Hybrid Friction Stir Channeling Technique to Improve the Cooling Efficiency of Electronic Components. Weld World, 62:497–509.

[3] Mehta, K.P., Vilaça, P., 2022, A Review on Friction Stir-based Channeling. Critical Reviews in Solid State and Materials Sciences, 47:1–45. https://doi.org/10.1080/10408436.2021.1886042.

[4] Thomas, W.M., Nicholas, E.D., Needham, J.C., Temple-smith, P., Kallee, S.W., Dawes, C.J., Friction stir welding, GB2306366A, 1997.

[5] Vilaça, P., Thomas, W., Friction Stir Welding Technology, in: P.M.G.P. Moreira, L.F. M. Da Silva, de C.M.S.T. Paulo (Eds.), Struct. Connect. Light. Met. Struct. Adv. Struct. Mater., 2011: pp. 85–124. https://doi.org/10.1007/8611.

[6] Çam, G., Javaheri, V., Heidarzadeh, A., 2023, Advances in FSW and FSSW of dissimilar Al-alloy plates. Journal of Adhesion Science and Technology, 37:162–194. https://doi.org/10.1080/01694243.2022.2028073.

[7] Ahmed, M.M.Z., El-Sayed Seleman, M.M., Fydrych, D., Çam, G., 2023, Friction Stir Welding of Aluminum in the Aerospace Industry: The Current Progress and State-of-the-Art Review. Materials (Basel), 16. https://doi.org/10.3390/ma16082971.

[8] Kashaev, N., Ventzke, V., Çam, G., 2018, Prospects of Laser Beam Welding AND Friction Stir Welding Processes for Aluminum Airframe Structural Applications. Journal of Manufacturing Processes, 36:571–600. https://doi.org/10.1016/j.jmapro.2018.10.005.

[9] Çam, G., İpekoğlu, G., 2017, Recent Developments in Joining of Aluminum Alloys. The International Journal of Advanced Manufacturing Technology, 91:1851–1866. https://doi.org/10.1007/s00170-016-9861-0.

[10] Vilaça, P., Gandra, J., Vidal, C., 2012, Linear Friction Based Processing Technologies for Aluminum Alloys: Surfacing, Stir Welding and Stir Channeling. Aluminium Alloys—New Trends in Fabrication and Applications, 159–197. https://doi.org/10.1016/j.colsurfa.2011.12.014.

[11] Karvinen, H., Aleni, A.H., Salminen, P., Minav, T., Vilaça, P., 2019, Thermal Efficiency and Material Properties of Friction Stir Channelling Applied to Aluminium Alloy AA5083. Energies, 12. https://doi.org/10.3390/en12081549.

[12] Gao, P., Zhang, Y., Mehta, K.P., 2020, Metallurgical and Mechanical Properties of Al–Cu Joint by Friction Stir Spot Welding and Modified Friction Stir Clinching. Metals and Materials International. https://doi.org/10.1007/s12540-020-00759-w.

[13] Mehta, K.P., Badheka, V.J., 2016, A review on Dissimilar Friction Stir Welding of Copper to Aluminum: Process, Properties, and Variants. Materials and Manufacturing Processes, 31:233–254. https://doi.org/10.1080/10426914.2015.1025971.

[14] Mehta, K.P., Badheka, V.J., 2017, Influence of Tool Pin Design on Properties of Dissimilar Copper to Aluminum Friction Stir Welding. Transactions of Nonferrous Metals Society of China (English Edition), 27. https://doi.org/10.1016/S1003-6326(17)60005-0.

[15] Mehta, K.P., Badheka, V.J., 2016, Effects of Tool Pin Design on Formation of Defects in Dissimilar Friction Stir Welding. Procedia Technology, 23:513–518. https://doi.org/10.1016/j.protcy.2016.03.057.

[16] Mehta, K.P., Badheka, V.J., 2017, Hybrid Approaches of Assisted Heating and Cooling for Friction Stir Welding of Copper to Aluminum Joints. Journal of Materials Processing Technology, 239:336–345. https://doi.org/10.1016/j.jmatprotec.2016.08.037.

[17] Patel, N.P., Parlikar, P., Dhari, R.S., Mehta, K., Pandya, M., 2019, Numerical Modelling on Cooling Assisted Friction Stir Welding of dissimilar Al-Cu joint. Journal of Manufacturing Processes, 47:98–109. https://doi.org/10.1016/j.jmapro.2019.09.020.

[18] Mehta, K.P., Badheka, V.J., 2016, Effects of Tilt Angle on the Properties Of Dissimilar Friction Stir Welding Copper to Aluminum. Materials and Manufacturing Processes, 31:255–263. https://doi.org/10.1080/10426914.2014.994754.

[19] Mehta, K.P., Badheka, V.J., 2015, Influence of Tool Design and Process Parameters on Dissimilar Friction Stir Welding of Copper to AA6061-T651 Joints. The International Journal of Advanced Manufacturing Technology, 80:2073–2082. https://doi.org/10.1007/s00170-015-7176-1.

[20] Elyasi, M., Taherian, J., Hosseinzadeh, M., Kubit, A., Derazkola, H.A., 2023, The Effect of Pin Thread on Material Flow and Mechanical Properties in Friction Stir Welding of AA6068 and Pure Copper. Heliyon, 9:e14752. https://doi.org/10.1016/j.heliyon.2023.e14752.

[21] Manickam, S., Rajendran, C., Balasubramanian, V., 2020, Investigation of FSSW Parameters on Shear Fracture Load of AA6061 and Copper Alloy Joints. Heliyon, 6:e04077. https://doi.org/10.1016/j.heliyon.2020.e04077.

[22] R.S. Mishra, Intergral channels in metal components and fabrication thereof, US006923362B2, 2005.

[23] Balasubramanian, N., Mishra, R.S., Krishnamurthy, K., 2008, Friction Stir Channeling: Characterization of the Channels. Journal of Materials Processing Technology, 209:3696–3704. https://doi.org/10.1016/j.jmatprotec.2008.08.036.

[24] Balasubramanian, N., Mishra, R.S., 2016, Development of a Mechanistic Model for Friction Stir Channeling. 54504 Journal of Manufacturing Science and Engineering, 132/1–4. https://doi.org/10.1115/1.4002453.

[25] Balasubramanian, N., Mishra, R.S., Krishnamurthy, K., 2011, Process Forces During Friction Stir Channeling in an Aluminum Alloy. Journal of Materials Processing Technology, 211:305–311. https://doi.org/10.1016/j.jmatprotec.2010.10.005.

[26] Vidal, C., 2014, Development and Mechanical Characterization of a New Manufacturing Palavras-chave Keywords.

[27] Vidal, C., Infante, V., Vilaça, P., 2020, Monitoring of the Mechanical Load and Thermal History During Friction Stir Channelling Under Constant Position and Constant Force Control Modes. Journal of Manufacturing Processes, 49:323–334. https://doi.org/10.1016/j.jmapro.2019.11.016.

[28] Vidal, C., Infante, V., Vilaça, P., 2019, Metallographic and Morphological Characterization of Sub-surface Friction Stirred Channels Produced on AA5083-H111. The International Journal of Advanced Manufacturing Technology, 105:2215–2235. https://doi.org/10.1007/s00170-019-04459-7.

[29] Vidal, C., Infante, V., Vilaça, P., 2013, Effect of Microstructure on the Fatigue Behavior of a Friction Stirred Channel Aluminium Alloy. Procedia Engineering, 66:264–273. https://doi.org/10.1016/j.proeng.2013.12.081.

[30] Vidal, C., Infante, V., Vilaça, P., 2015, Characterisation of Fatigue Fracture Surfaces of Friction Stir Channelling Specimens Tested at Different Temperatures. Engineering Failure Analysis, 56:204–215. https://doi.org/10.1016/j.engfailanal.2015.02.009.

[31] Vidal, C., Infante, V., 2014, Role of Friction Stir Channel Geometry on the Fatigue Behaviour of AA5083-H111 at 120°C and 200°C. Advanced Materials Research, 891–892:1494–1499. https://doi.org/10.4028/www.scientific.net/AMR.891-892.1494.

[32] J. Gandra, Methods and appratus for creating channels in workpieces, WO 2018/083438 A1, 2018.

[33] Gandra, J., 2019, Integration of Thermal Managements Networks into Aluminium Structures by Stationary Shoulder Friction Stir Channelling. 6th Int Conf Sci Tech Adv Frict Stir Weld Process, Louvain-Louisiana-Neuve (Belgium), 1⟨https://sites.uclouvain.be/fswp2019/presentations.php?ind=893⟩.

[34]. ThyssenKrupp Materials (UK) Ltd, Aluminium Alloy 5083-O H111 - Material Data Sheet, 2023.

[35] Warlimont, H., Martienssen, W., Springer Handbook of Materials Data, 2018.

[36] Metalcenter Group Oy Ab, EN Cu-OF/CW008A 99,95% pure copper - Data sheet, 2023.

[37] Specific heat from A. Bejan, A. D. Kraus, Heat Transfer Handbook, 2003.

[38] Oliver, W.C., Pharr, G.M., 1992, An Improved Technique for Determining Hardness and Elastic Modulus Using Load and Displacement Sensing Indentation Experiments. Journal of Materials Research, 7:1564–1583.

[39] Balasubramanian, N., Krishnamurthy, K., Mishra, R.S., 2007, Preliminary Study of Pressure Drop and Heat Transfer Through a Friction Stir Channel. ASME 2007 International Mechanical Engineering Congress and Exposition, 933–939. https://doi.org/10.1115/IMECE2007-41634.

[40] Pandya, S., Gurav, S., Hedau, G., Saha, S., Arora, A., 2020, Effect of Axial Conduction in Integral rough Friction Stir Channels: Experimental Thermo-Hydraulic Characteristics Analyses. Heat and Mass Transfer. https://doi.org/10.6013/jbrewsocjapan1915.62.477.

[41] Pandya, S., Mishra, R.S., Arora, A., 2019, Channel Formation During Friction Stir Channeling Process — A Material Flow Study Using X-Ray Micro-computed Tomography and Optical Microscopy. Journal of Manufacturing Processes, 41:48–55. https://doi.org/10.1016/j.jmapro.2019.03.021.

[42] Heidarzadeh, A., Mironov, S., Kaibyshev, R., Çam, G., Simar, A., Gerlich, A., Khodabakhshi, F., Mostafaei, A., Field, D.P., Robson, J.D., Deschamps, A., Withers, P.J., 2020, Friction Stir Welding/processing of Metals and Alloys: A Comprehensive Review on Microstructural Evolution. Progress in Materials Science, 117:100752. https://doi.org/10.1016/j.pmatsci.2020.100752.

[43] Vidal, C., Infante, V., Vilaça, P., 2014, Fatigue Behaviour at Elevated Temperature of Friction Stir Channelling Solid Plates of AA5083-H111 Aluminium Alloy. International Journal of Fatigue, 62:85–92. https://doi.org/10.1016/j.ijfatigue.2013.10.012.

[44] Vidal, C., Infante, V., Vilaça, P., 2014, Fatigue Assessment of Friction Stir Channels. International Journal of Fatigue, 62:77–84. https://doi.org/10.1016/j.ijfatigue.2013.10.009.

[45] Vidal, C., Infante, V., Vilaça, P., 2012, Mechanical Characterization of Friction Stir Channels Under Internal Pressure and In-plane Bending. Key Engineering Materials, 488–489:105–108. https://doi.org/10.4028/www.scientific.net/KEM.488-489.105.

[46] Mehta, K.P., Patel, R., Vyas, H., Memon, S., Vilaça, P., 2020, Repairing of Exit-hole in Dissimilar Al-Mg Friction Stir Welding: Process and Microstructural Pattern. Manufacturing Letters, 23:67–70. https://doi.org/10.1016/j.mfglet.2020.01.002.

[47] Mehta, K.P., 2019, A Review on Friction-based Joining of Dissimilar Aluminum – Steel Joints. Journal of Materials Research, 34:78–96. https://doi.org/10.1557/jmr.2018.332.

[48] Ólafsson, D., Vilaça, P., Vesanko, J., 2020, Multiphysical Characterization of FSW of Aluminum Electrical Busbars with Copper Ends. Weld World, 64:59–71. https://doi.org/10.1007/s40194-019-00814-0.

[49] Mehta, K.P., Carlone, P., Astarita, A., Scherillo, F., Rubino, F., 2019, Conventional and Cooling Assisted Friction Stir Welding of AA6061 and AZ31B Alloys. Materials Science and Engineering: A, 759:252–261. https://doi.org/10.1016/j.msea.2019.04.120.

[50] H. Okamoto, M.E. Schlesinger, E.M. Mueller, ASM Handbook Volume 3: Alloy Phase Diagrams - ASM International, 1992. http://www.asminternational.org/online-catalog/handbooks/-/journal%7B_%7Dcontent/56/10192/06479G/PUBLICATION.